REverse-transcriptase ACTivity with CRISPR (REACTR) Assay for Rapid and User-Friendly Therapeutic Drug Monitoring in Cytomegalovirus Care

Willow A. Chernoske[1], Maya A. Singh[1], Carrie H. Lin[1], Megan M. Chang[1], Cosette A. Craig[2], Albert H. Park,[3,4] Joseph E. Rower[5], Ayokunle O. Olanrewaju[1,2]

Author Affiliations:

1. Department of Bioengineering, Seattle, WA, 98195
2. Department of Mechanical Engineering, University of Washington, Seattle, WA, 98195
3. Department of Otolaryngology-Head and Neck Surgery, University of Utah, Salt Lake City, UT, 84112
4. Department of Pediatrics, University of Utah, Salt Lake City, UT, 84112
5. Center for Human Toxicology, Department of Pharmacology and Toxicology, University of Utah, Salt Lake City, UT, 84112

Corresponding author: Ayokunle Olanrewaju, ayokunle@uw.edu

Abstract

Background: Cytomegalovirus (CMV) can cause severe disease and death in infants and immunocompromised people. Although effective at treating CMV, the first-line drug – ganciclovir (GCV) – has high rates of pharmacokinetic variability which leads to significant rates of underexposure or toxicity. Intracellular concentrations of ganciclovir triphosphate (GCV-TP) – GCV's active anabolite – are associated with dose-dependent neutropenia and could enable dose individualization to improve treatment efficacy and reduce adverse effects. However, GCV-TP is currently measured using liquid chromatography tandem mass spectrometry (LC-MS/MS) which is impractical for routine use, especially in resource-limited settings, because of its high cost, labor-intensiveness, and need for specialized equipment. To address this gap, we adapted the REverse transcriptase ACTivity with CRISPR (REACTR) assay to measure GCV-TP.

Methods: We leveraged our earlier work using REACTR to measure reverse transcriptase (RT) inhibitors used to treat and prevent human immunodeficiency virus (HIV) because GCV-TP serendipitously also inhibits HIV RT. We designed custom DNA templates, primers, and CRISPR complexes to accurately measure GCV-TP spiked into buffer and blood. We evaluated the assay's analytical performance with 40 dried blood spots from infants with congenital CMV.

Results: REACTR reproducibly measured clinically relevant GCV-TP concentrations using a simple workflow and equipment that are readily available in many clinical laboratories. REACTR measurements of clinical samples correlated with LC-MS/MS GCV-TP measurements ($r = -0.7891$; $p<0.0001$).

Conclusions: This study highlights the potential of REACTR as a rapid and accessible alternative to LC-MS/MS for therapeutic drug monitoring of GCV.

Keywords

Cytomegalovirus, Ganciclovir, Therapeutic Drug Monitoring, CRISPR, Assay, Point-of-care, Enzyme Activity Assay

Human cytomegalovirus (CMV) is a herpesvirus with an estimated global seroprevalence of over 80% [1]. While infection is typically asymptomatic in immunocompetent individuals, CMV can cause life-long morbidities and even death in immunocompromised or immuno-immature populations like transplant recipients or infants. Congenital CMV (cCMV) affects approximately 1 in 200 newborns, with 10-20% of infants with cCMV exhibiting symptoms at birth [2], [3]. 50% of children with cCMV symptoms at birth suffer from long-term hearing loss, developmental delay, or neurocognitive impairment [4]. Moreover, as many as 10% of infants with symptomatic cCMV die in early infancy due to the disease [3], [5]. Like other herpesviruses, CMV causes an incurable, life-long infection that can become dormant and reactivate over time [6]. While there has been interest in developing CMV vaccines since the 1970s, no CMV vaccine has been licensed to date [7], [8].

Ganciclovir (GCV) and its oral pro-drug valganciclovir (VGCV) serve as the first-line antiviral agents for symptomatic CMV treatment [3]. GCV, or 9-(1,3-dihydroxy-2-propoxymethyl)guanine, is an acyclic guanosine analog that potently inhibits the replication of herpesviruses [9]. Upon cellular uptake, GCV is phosphorylated into its active form, ganciclovir triphosphate (GCV-TP), by viral and host kinases [10]. GCV-TP works by selectively inhibiting extension of viral DNA by herpesvirus DNA polymerases, such as UL54 polymerase [11]. Although effective, GCV therapy is plagued by substantial interindividual variability in drug exposure and high rates of toxicity. With standard dosing, underexposure and inadequate treatment occur in an estimated 30% of infants [12], while overexposure and significant toxicity occur in 25% of infants [13]. These challenges underscore the need for therapeutic drug monitoring (TDM) of GCV to guide personalized dosing.

Current TDM of GCV measures plasma or serum GCV concentrations and is performed using liquid chromatography tandem mass spectrometry (LC-MS/MS) or high-performance liquid chromatography (HPLC) [14]. These tests provide sensitive and accurate GCV measurement but require expensive, centralized equipment and highly trained personnel. Alternative methods for measuring plasma GCV concentrations include Raman spectroscopy, capillary electrophoresis, and electrochemical sensing, but LC-MS/MS remains the gold standard in clinical studies and routine care [14], [15], [16], [17]. Furthermore, clinical studies using LC-MS/MS or HPLC methods for plasma GCV monitoring have presented conflicting evidence for the effectiveness of plasma GCV TDM as a biomarker for treatment optimization [12], [14], [18], [19], [20], [21], [22], [23]. While some studies have reported associations between plasma GCV

81 exposure and treatment outcomes and even target therapeutic ranges for monitoring [19], [20],
82 [24], others have found no such relationship [21], [22], with results varying by study and patient
83 population. As a result, experts have called for further exploration of GCV-TP – GCV's active
84 intracellular anabolite – as a biomarker for TDM, as it may better predict toxicity and treatment
85 response [22], [25], [26], [27].
86
87 A 2015 study demonstrated that intracellular GCV-TP concentrations in kidney transplant
88 recipients were significantly correlated with neutrophil count [22]. In the same study, no
89 associations were seen between plasma GCV or other metabolites of the drug and neutrophil
90 count, suggesting that GCV-TP may be unique in its ability to predict neutropenia. This is the
91 only study of its kind correlating intracellular GCV derivatives with treatment outcomes, likely
92 due to the current cost and complexity associated with GCV-TP measurement. Intracellular
93 GCV-TP concentrations have so far only been measured using LC-MS/MS, a method that
94 requires a complex, multistep procedure to separate GCV-TP from other GCV derivatives
95 before mass spectrometry measurements [28]. This intensive procedure and the increased
96 complexity, time, and equipment associated with GCV-TP measurement make it highly
97 centralized and limit widespread use.
98
99 We recently developed the REverse transcriptase ACTivity with CRISPR (REACTR) assay for
100 rapid and minimally instrumented measurement of reverse transcriptase (RT) inhibitors used in
101 human immunodeficiency virus (HIV) treatment and prevention [29], [30], [31], [32], [33].
102 REACTR measures intracellular concentrations of nucleotide analog drugs based on inhibition
103 of DNA synthesis by HIV RT enzyme. Complementary DNA (cDNA) synthesized by HIV RT
104 from a custom DNA template activates a Cas12-crRNA complex, triggering collateral cleavage
105 of DNA reporter molecules. Nucleotide RT inhibitors (NRTIs) compete for incorporation into
106 cDNA with deoxynucleotide triphosphates (dNTPs), such that chain termination, cDNA
107 synthesis, and resulting fluorescence from activated CRISPR complexes are proportional to the
108 NRTI concentration in the reaction. GCV-TP, despite canonically targeting herpesvirus DNA
109 polymerases, also inhibits HIV RT via delayed chain termination [34], [35]. Consequently, while
110 REACTR was originally developed for measuring HIV medications, GCV-TP's inhibition of HIV
111 RT allowed us to adapt REACTR to measure GCV-TP.
112
113 In this study, we adapted the REACTR assay for measuring GCV-TP in buffer and dried blood
114 spots (DBS) and evaluated the assay's analytical performance with DBS from a clinical

115 pharmacokinetic (PK) trial. We first designed custom DNA templates and optimized assay
116 conditions for detecting GCV-TP spiked into buffer and blood matrices, characterized its
117 sensitivity and reproducibility, and then validated its performance using clinical DBS samples
118 from the Randomized Controlled Trial of Valganciclovir for Cytomegalovirus Infected Hearing
119 Impaired Infants (ValEAR) study (ClinicalTrials.gov #NCT03107871) [36]. Finally, we compared
120 REACTR GCV-TP measurements with those obtained by LC-MS/MS to assess concordance
121 with the gold-standard method.

122 RESULTS AND DISCUSSION

123 Adapting REACTR for measuring GCV-TP

124 REACTR uses a ssDNA template with a primer binding region followed by a repeat region
125 specific to the nucleotide analog drug of interest, a complementary crRNA recognition region, a
126 PAM sequence, and a poly T tail (**Figure 1A**). To adapt REACTR to measure GCV-TP, a
127 guanine analog, a cytidine repeat region was incorporated into the template. Assays were run
128 with the DNA template, a reverse primer, RT, dNTPs, a Cas12a-crRNA complex specific to the
129 DNA template, DNA reporters with fluorophore-quencher pairs, and sample containing GCV-TP
130 (**Figure 1B, Table S1**). As in previous demonstrations of REACTR, as the amount of drug in the
131 sample increases, DNA chain termination increases [33]. This prevents synthesis of the crRNA
132 recognition region and results in reduced fluorescence (**Figure 1B**). Thus, we can infer GCV-TP
133 drug concentrations based on REACTR assay fluorescence.

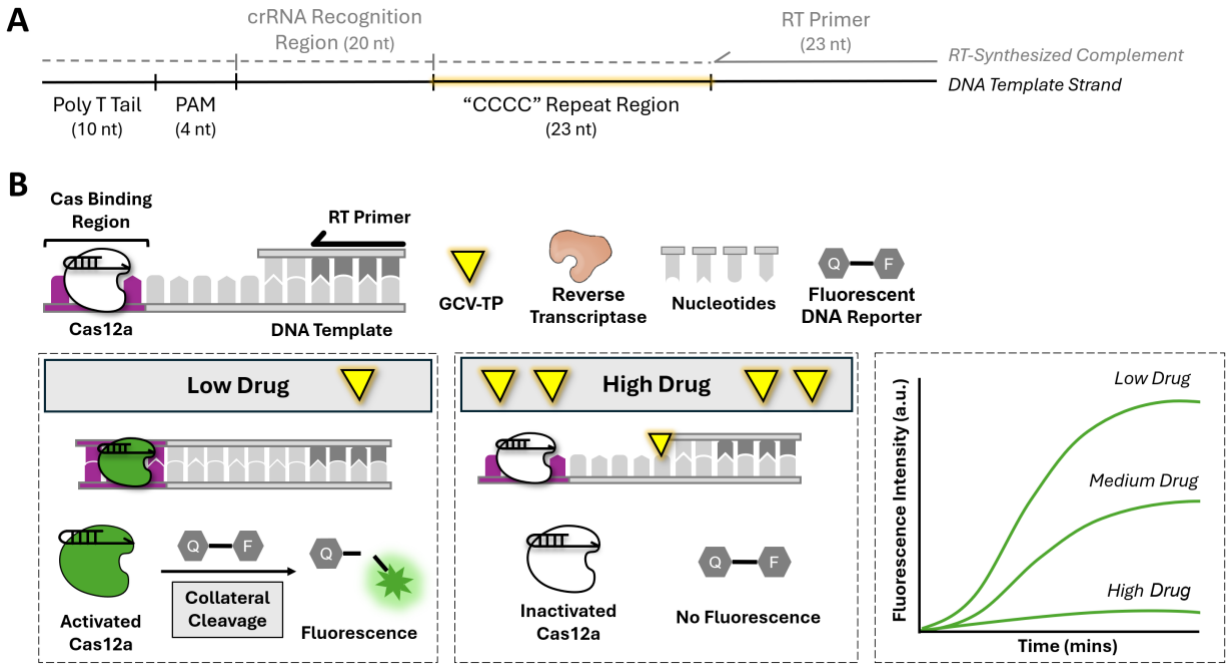

134

135 **Figure 1. Overview of the REverse transcriptase ACTivity with CRISPR (REACTR) assay**
136 **for measuring GCV-TP based on its inhibition of DNA synthesis by HIV RT enzyme.** (**A**)
137 The REACTR template optimized for measuring GCV-TP (a guanine analog) includes a primer
138 binding region followed by a cytidine repeat region, a complementary crRNA recognition region,
139 a PAM sequence, and a poly T tail. (**B**) At low drug concentrations, HIV RT can synthesize full-
140 length DNA with CRISPR binding regions that activate Cas12a complexes that cleave DNA
141 reporters leading to fluorescence. Conversely, at high drug concentrations, DNA chain
142 termination occurs and inactivated Cas12a complexes are unable to generate fluorescence.
143
144 **REACTR can measure clinically relevant GCV-TP concentrations in buffer**
145 We assessed REACTR's ability to measure clinically relevant GCV-TP concentrations by
146 spiking the drug into aqueous buffer at concentrations from 0.1 mM to 0.01 nM and added the
147 spiked solutions into REACTR assays. Real-time measurements showed decreased
148 fluorescence as GCV-TP concentration increased (**Figure 2A, Figure S1A**). We explored the
149 role of template design on REACTR's sensitivity to GCV-TP by running the assay with a
150 template containing a "CCCC" repeat region designed to bind GCV-TP (a guanine analog) and
151 a "TTTA" repeat region originally designed for tenofovir diphosphate (an adenine analog used in
152 HIV treatment) (**Figure 2B, Figure S1B**). The "CCCC" template had a 50% Inhibitory
153 Concentration (IC_{50}) (95% Confidence Interval [CI]) of 10.8 nM (9.1 to 12.9 nM), while the
154 "TTTA" template required at least 3 orders of magnitude greater GCV-TP concentrations before
155 inhibition was observed and did not provide a quantifiable IC_{50} within the span of concentrations
156 tested. These results, in agreement with our past work, show that REACTR assay parameters
157 like DNA template sequence can be tuned to specifically measure clinically relevant levels of
158 different antiviral drugs.
159
160 We also explored the role of reaction incubation time on REACTR assays with GCV-TP by
161 generating enzyme inhibition curves at the 15-, 30-, 60-, and 90-minute time points (**Figure 2C**).
162 As expected, raw fluorescence signal increased as assay incubation time increased.
163 Normalizing data showed that the IC_{50} (95% CI) of GCV-TP at 15, 30, 60, and 90 min were 3.9
164 nM (N/A to 6.5 nM), 5.2 nM (4.3 to 6.4 nM), 10.8 nM (9.1 to 12.9 nM), and 35.4 nM (29.9 to 42.6
165 nM), respectively (**Figure 2D**). Thus, there is a tradeoff between the assay fluorescence signal
166 intensity and the ability to detect low concentrations of GCV-TP.

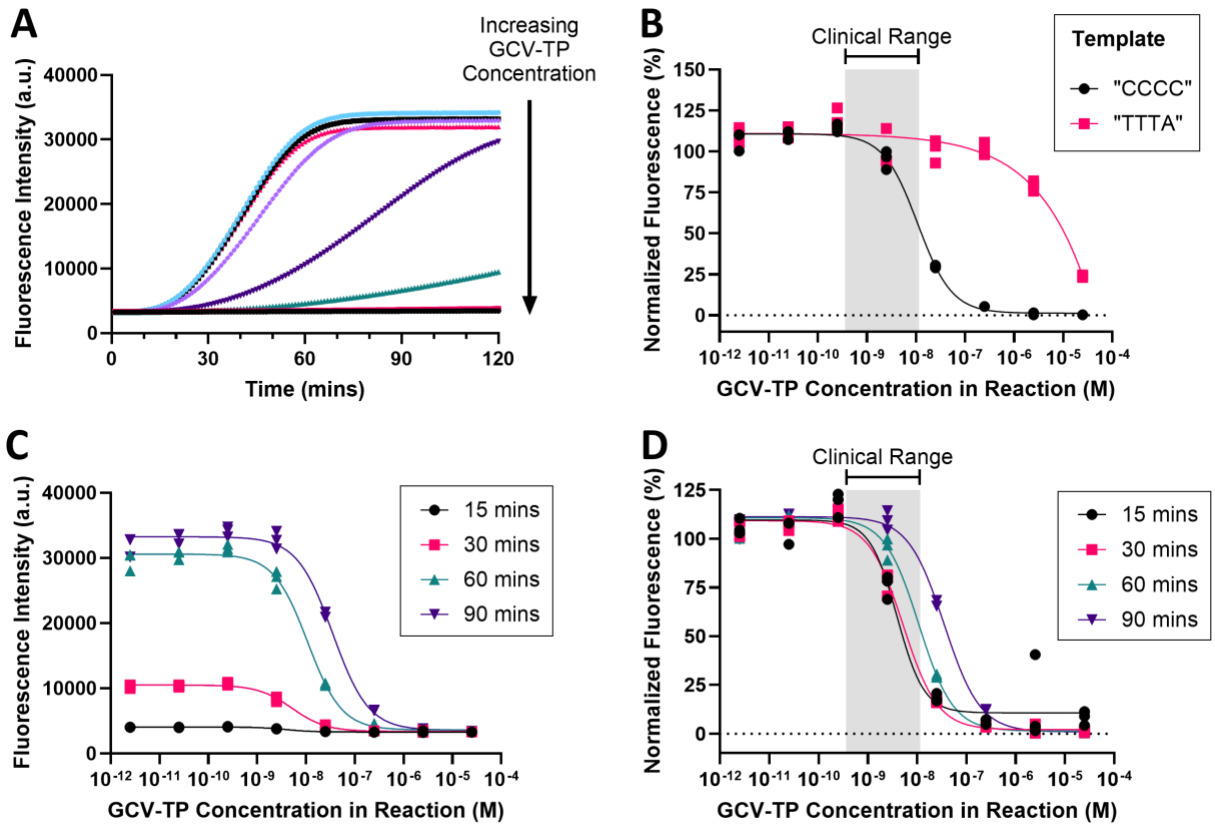

Figure 2. REACTR sensitively and specifically measures varying concentrations of GCV-TP spiked in buffer. (**A**) Mean real-time REACTR curves using "CCCC" templates with varying concentrations of GCV-TP spiked in buffer. (**B**) Normalized RT inhibition curves for GCV-TP in REACTR assays using templates with either "CCCC" or "TTTA" repeat regions show specificity in detecting the guanine analog drug using the cytidine-enriched template. (**C**) RT inhibition curves for GCV-TP at various timepoints – extracted from raw data in (A) – show an increase in fluorescence signal as assay incubation time increases. (**D**) Normalized RT inhibition curves for GCV-TP at various timepoints show that shorter assay incubation times enable detection of lower GCV-TP concentrations. n = 3 technical replicates. Gray regions indicate the clinical range of GCV-TP (0.362 to 11.5 nM) in DBS of infants with cCMV.

REACTR accurately measures clinically relevant GCV-TP concentrations spiked in DBS

We next adapted REACTR to measure GCV-TP in DBS as a convenient way to test archived clinical samples. Using DBS from healthy donors not receiving any antiviral drugs, we developed a simple sample preparation workflow that used thermolabile proteinase K (TPK) and heat to denature blood proteins (**Figure 3**). GCV-TP was spiked into blood eluted from DBS at concentrations from 0.1 mM to 0.01 nM prior to the addition of TPK and heat. The dilution and

185 protein denaturation steps in the sample preparation process reduce non-specific inhibition of
186 HIV-RT by blood matrix components including hemoglobin and immunoglobulins.

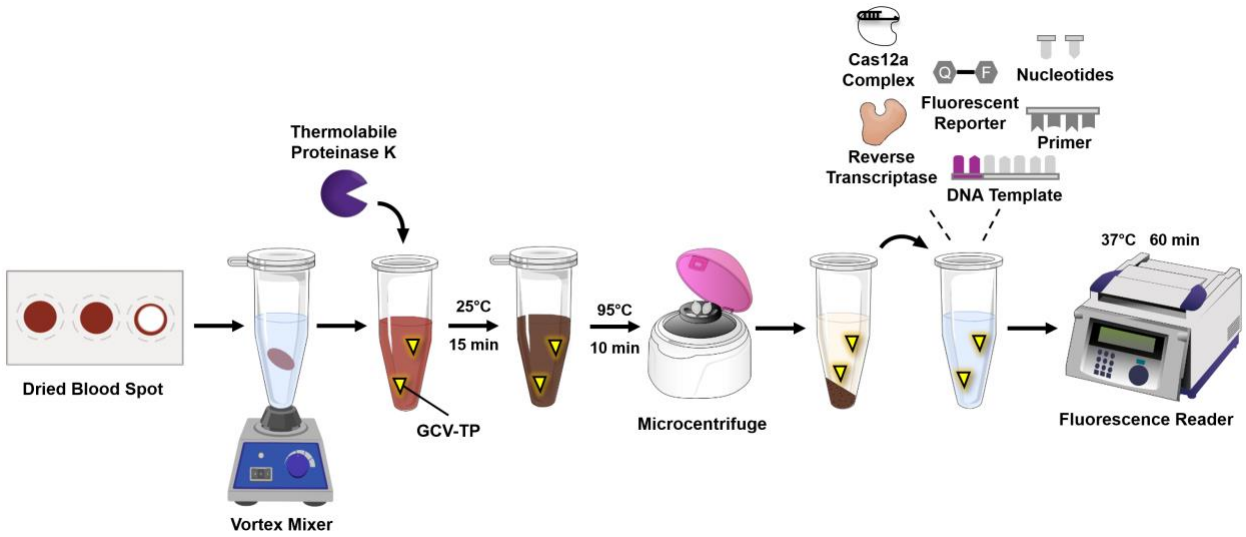

187

188 **Figure 3. Simple sample preparation workflow for measuring antiviral drugs in DBS using**
189 **the REACTR enzymatic assay.** DBS punches are vortex mixed in water to lyse red blood cells
190 and release intracellular nucleotide analogs, then treated with thermolabile proteinase K to
191 digest blood proteins, followed by heat denaturation. The supernatant with extracted GCV-TP is
192 then added to a tube with RT, DNA template, primer, Cas12a complex, fluorescent reporter, and
193 nucleotides, then incubated at 37°C for 60 minutes in a fluorescence reader.

194

195 We found that, even with our sample preparation process, the maximum signal intensity (from
196 "no drug" controls) and the assay variation increased with REACTR in DBS compared to buffer
197 (**Figure S2**). Although in Figure 2D a 30-minute incubation time with REACTR in buffer provided
198 inhibition curves that enabled GCV-TP quantification within the clinical range, we chose a 60-
199 minute assay time with REACTR in DBS to improve assay performance. At a 30-minute
200 incubation time, the decrease in the maximum signal intensity with REACTR in DBS compared
201 to REACTR in buffer was 46.2% and the coefficient of variation (CV) of "no drug" controls in
202 DBS was 8.8% compared with 4.4% in buffer (**Figure S2B-D**). Meanwhile, at a 60-minute
203 incubation time, the maximum signal intensity decreased by 40.7% in DBS compared to buffer,
204 and the CV of "no drug" controls was 3.7% in DBS compared with 3.1% in buffer (**Figure 4A**).
205 We attribute these differences in performance between REACTR in DBS and buffer to
206 incomplete elimination of blood matrix effects with our relatively simple sample preparation
207 process. Nevertheless, we prioritized assay simplicity and the use of instruments that are
208 typically available in most clinical laboratories (vortexer, heat block, microcentrifuge, and

209 fluorescence reader) for all our assay preparation and readout. Despite the decrease in raw
210 signal intensity, the normalized inhibition curve for GCV-TP spiked in DBS closely mirrored that
211 seen in buffer at 60 minutes, with a modest rightward shift in IC_{50} between buffer (10.8 nM, 95%
212 CI = 9.09 to 12.9 nM) and blood (21.2 nM, 95% CI = 15.6 to 28.8 nM) (**Figure 4B**).

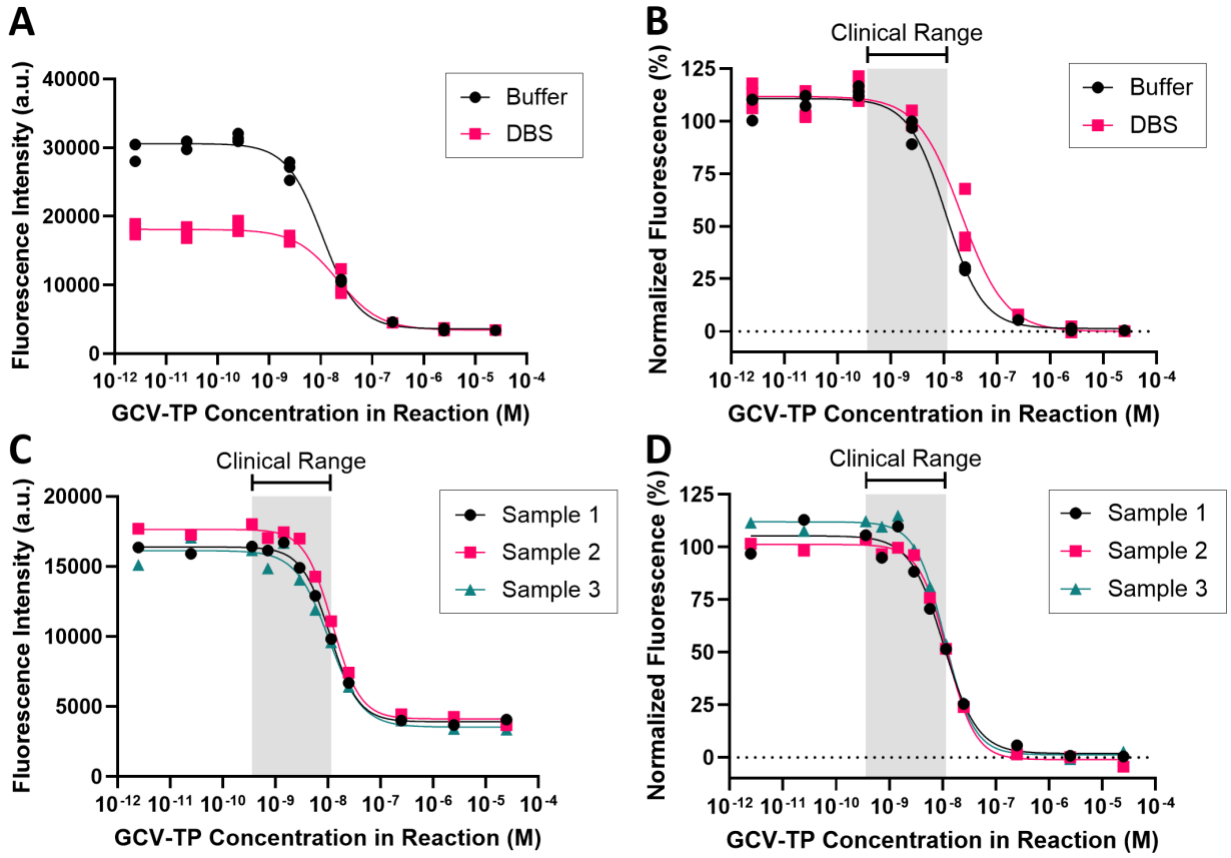

213

214 **Figure 4. REACTR provides consistent results with GCV-TP spiked in DBS.** (**A**) RT-
215 inhibition curve with varied GCV-TP concentrations shows significantly lower maximum
216 fluorescence signal with spiked DBS compared with spiked buffer at a 60-minute assay
217 incubation time. n = 3 technical replicates. (**B**) Normalized inhibition curve for GCV-TP spiked in
218 buffer and DBS – extracted from data in (A) – showing excellent agreement between buffer and
219 blood with a slight rightward shift for the assay in DBS. (**C**) RT inhibition curves for GCV-TP
220 spiked in blood from 3 independent blood samples show excellent agreement across samples.
221 Each point on the curve represents the mean of 3 technical replicates. (**D**) Normalized 60-
222 minute RT inhibition curves for GCV-TP spiked in 3 independent blood samples – extracted
223 from data in (C) – show excellent consistency across samples.

224

225 We evaluated sample-to-sample variation using spiked DBS samples generated from
226 independent blood samples not containing any antiviral drugs (**Figure 4C-D, Figure S3**). Both

227 raw fluorescence curves (**Figure 4C**) and normalized curves (**Figure 4D**) were highly consistent
228 across samples. Across the three samples, the average intra-assay CV was 12.8% and the
229 inter-assay CV was 10.6%. We also calculated the Z' score to assess the assay's ability to
230 distinguish between positive and negative controls and as an indicator of its suitability for high
231 throughput screening [42]. The average intra-assay Z' score was 0.54 and the inter-assay Z'
232 score was 0.56 – both above the quality cutoff of 0.5 for Z' value typically used in high-
233 throughput screening assays.
234
235 We also evaluated the assay's ability to distinguish drug concentrations in the clinical range
236 from the "no drug" control. Of the sampled concentrations within the clinical range, the raw
237 fluorescence became significantly different from "no drug" control at the 5.8 nM drug condition
238 ($p = 0.0214$) when assessed with a one-way ANOVA with multiple comparisons. The same
239 cutoff was seen after normalizing fluorescence ($p = 0.0001$). This indicates that the assay in its
240 current form can detect GCV-TP concentrations at the upper end of the clinical range (0.362 to
241 11.5 nM GCV-TP) in DBS, which may be useful for detecting potentially toxic concentrations of
242 GCV-TP in blood.
243
244 **REACTR measurements correlate with LC-MS/MS-measured GCV-TP concentrations**
245 To assess performance of the REACTR assay with clinical samples, we tested 40 DBS samples
246 collected from 16 infants enrolled in the ValEAR trial with GCV-TP concentrations ranging from
247 0 to 1891 fmol/6 mm punch. **Figure 5** shows REACTR fluorescence intensity measurements
248 compared with LC-MS/MS GCV-TP concentrations from the ValEAR study. REACTR
249 measurements of the clinical DBS samples correlated with LC-MS/MS measurements of GCV-
250 TP ($n = 40$, Pearson $r = -0.7891$; $p < 0.0001$; 95% confidence interval (CI) = -0.8834 to -0.6332),
251 with a coefficient of determination (r^2) of 0.6226. LC-MS/MS correlations to raw fluorescence
252 values and normalized values (**Figure S3**) were highly consistent. These initial results
253 demonstrate the potential of REACTR to provide accurate GCV-TP measurements at a fraction
254 of the time, cost, and complexity required for LC-MS/MS testing.

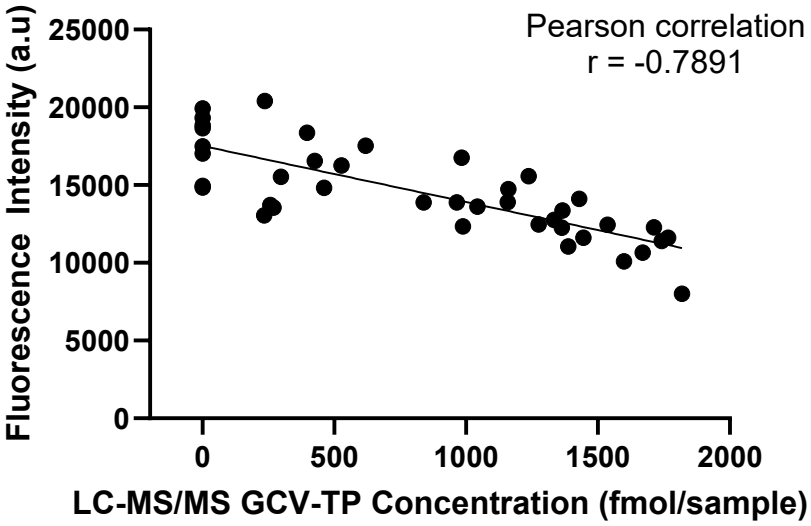

255

256 **Figure 5. REACTR results correlate with LC-MS/MS GCV-TP concentrations in DBS from**
257 **a clinical pharmacokinetic trial.** n = 40 DBS from infants with cCMV. Each point represents
258 the mean of 3 technical replicates.

259

260 **Limitations and future directions**

261 While this study demonstrates the feasibility of adapting REACTR for intracellular GCV-TP
262 monitoring, several limitations exist. First, the current assay is limited to detecting GCV-TP
263 levels at the upper end of the clinical range. Improving assay sensitivity through reagent
264 optimization and enhanced sample preparation or readout methods will be important to expand
265 detection to the lower end of the clinical range. We previously developed and validated a
266 mathematical model showing that increasing DNA template length, increasing the number of
267 potential chain termination events by enriching for the complement of the drug in the DNA
268 template, and decreasing the concentration of competing nucleotides are all effective strategies
269 for increasing the analytical sensitivity of assays like REACTR [31]. Switching from using HIV
270 RT to the UL54 polymerase, the canonical target of GCV-TP, may also improve the assay's
271 sensitivity to lower concentrations of the drug. Exploring alternate sample preparation or readout
272 strategies that reduce the influence of blood matrix effects without sacrificing assay simplicity
273 would also help to improve the performance of the assay. Second, clinical validation was
274 performed using DBS from a relatively small cohort of infants with cCMV. Although REACTR
275 measurements correlated with LC-MS/MS, larger studies will be necessary to establish assay
276 reproducibility and to correlate GCV-TP levels with treatment response and toxicity outcomes.
277 Third, the optimization and clinical validation shown here focused exclusively on infants with

278 cCMV. GCV is also used widely in transplant recipients who may exhibit different
279 pharmacokinetic profiles and thus may have a different clinical range. In future work we hope to
280 validate our assay for measuring GCV-TP in DBS from transplant populations to broaden
281 clinical utility.
282
283 **Conclusion**
284 This study validates the REACTR platform for measuring intracellular GCV-TP, the active
285 metabolite of GCV used in the treatment of CMV infection. By leveraging GCV-TP's ability to
286 inhibit HIV RT and coupling changes in cDNA synthesis by HIV RT to Cas12a-based detection,
287 REACTR measures clinically relevant concentrations of GCV-TP in DBS samples in 60 minutes.
288 REACTR was highly reproducible in DBS across independent blood samples, with average
289 intra-assay and inter-assay CVs of 12.8% and 10.6%, respectively, and intra-assay and inter-
290 assay Z' scores above 0.5. Importantly, REACTR measurements of clinical DBS samples from
291 infants living with cCMV correlated with LC-MS/MS measurements of GCV-TP ($r = -0.7891$; $p <$
292 0.0001), demonstrating agreement with the current gold-standard analytical method. Compared
293 to LC-MS/MS, REACTR offers several advantages: (1) streamlined sample preparation, (2)
294 reduced turn-around time, and (3) use of commonly available and relatively inexpensive
295 laboratory equipment. These features could enable expanded access to therapeutic drug
296 monitoring of GCV-TP, which has been called for but not widely implemented due to the
297 limitations and associated costs/complexities of current techniques. Future work will prioritize
298 improving assay sensitivity through reaction chemistry and workflow optimization and
299 conducting larger clinical validation studies across both cCMV and transplant populations.
300 Taken together, our results demonstrate the feasibility of REACTR as a rapid, accessible, and
301 cost-effective approach for monitoring GCV-TP levels with the potential for use in clinical trials
302 and/or routine care.

303 MATERIALS AND METHODS

304 **REACTR assay workflow**
305 REACTR workflows were adapted from a previously described method by Singh et al. [33]. The
306 Cas12a-crRNA complex was created by incubating 100 nM LbCas12a (M0653T, New England
307 Biolabs) and 100 nM crRNA (Integrated DNA Technologies) in REACTR buffer containing 50
308 mM Tris-HCl (77-86-1, Sigma-Aldrich) at pH 8, 50 mM Potassium Chloride (KCl) (60142-100
309 ML-F, Sigma-Aldrich), 15 mM Magnesium Chloride (MgCl2) (7786-30-3, Sigma-Aldrich), 7 mM

310 dithiothreitol (DTT) (3483-12-3, Sigma-Aldrich), and 0.06% Triton X-100 (9036-19-5, Sigma-
311 Aldrich) for 15 minutes at 25℃.
312
313 For spiked buffer experiments, GCV-TP (NC2174868, Axxora) was diluted in nuclease-free
314 water at varying concentrations from 0.1 mM to 0.01 nM. 40 µL REACTR assays containing 10
315 µL of sample or drug dilution, 25 nM Cas12-crRNA complex, 25 nM dNTPs, 0.5 nM DNA
316 template, 12.5 nM primer, 500 nM fluorescent reporter (Integrated DNA Technologies), and 0.04
317 units/µL of HIV RT (LS005009, Worthington Biochemical) in REACTR buffer were added to 96-
318 well armadillo PCR plates (Thermo Scientific, AB2396). dNTP and template concentrations
319 were chosen to maximize sensitivity to GCV-TP via decreased competition of dNTPs while
320 maintaining signal intensity [31]. All assays were run against "no-drug" positive controls and "no-
321 enzyme" negative controls. Reactions were incubated at 37℃ in a thermal cycler (Bio Rad
322 CFX96 Touch Real-Time PCR Detection System) for 60 to 120 minutes. Fluorescence
323 measurements were taken every minute during the incubation period. Raw and analyzed data is
324 available on Zenodo [37].
325
326 **DBS sample preparation**
327 6 mm DBS punches were collected in 1.7 mL Eppendorf tubes and eluted with 67.5 µL of
328 nuclease free water. The tube was then vortexed for 1 minute and centrifuged in a
329 microcentrifuge for 30 seconds. Eluted blood was transferred to a separate tube and
330 thermolabile proteinase K (P8111L, NEB) was added to create a final concentration of 25%
331 blood and 2.5% proteinase K. The tube was gently mixed before being incubated at 25℃ for 15
332 minutes followed by a heat inactivation step at 95℃ for 10 minutes. The tube was centrifuged
333 again in a microcentrifuge for 1 minute to pellet proteinaceous material. The supernatant was
334 then added to the REACTR assay.
335
336 For spiked DBS experiments, GCV-TP was diluted in nuclease-free water (H_2O) at varying
337 concentrations from 1 mM to 0.1 nM and added to eluted DBS punches at a ten-fold dilution
338 prior to the proteinase K. The elution volume in spiked DBS experiments was reduced
339 accordingly to maintain a final concentration of 25% blood and 2.5% proteinase K. Remaining
340 sample preparation was performed as described above. Sample to sample variation was
341 assessed using three independent blood samples. Sample 1 was derived from pooled blood
342 purchased from BioIVT, and samples 2 and 3 were from independent donors not receiving
343 GCV.

344

345 **Clinical DBS sample collection**

346 Authentic clinical DBS samples were obtained from the ValEAR trial, a randomized, multicenter,
347 placebo-controlled clinical trial of VGCV in infants with a positive CMV test [38]. The trial was
348 conducted under central institutional review board (IRB) approval (University of Utah/Primary
349 Children's Hospital board; cIRB_00090760, NCT03107871) and in accordance with the
350 Declaration of Helsinki. Infants were enrolled with informed parental consent and randomized to
351 receive VGCV (16 mg/kg twice daily for 6 months) or placebo. Monthly venipuncture blood
352 samples were collected for PK analyses. DBS samples were stored at –80°C until analysis.

353

354 **LC-MS/MS Analysis of GCV-TP**

355 LC-MS/MS quantification of GCV-TP in DBS samples is described by Lindquist-Kleissler et al.
356 and adapts previously described methods [36], [39], [40], [41]. Briefly, each 6 mm DBS punch
357 was extracted into 0.5 mL of 70% methanol (MeOH) in H_2O by sonication for 15 minutes. GCV-
358 TP in the supernatant was fractionated from other phosphorylated species using Waters QMA
359 solid phase extraction (SPE) cartridges, followed by dephosphorylation with acid phosphatase
360 and cleanup using a Phenomenex Strata-X SPE cartridge. A 30 µL aliquot of each sample was
361 then injected onto a TSQ Vantage triple quadrupole mass spectrometer (ThermoScientific)
362 interfaced with an Accela UHPLC pump and autosampler (ThermoScientific). Chromatographic
363 separation was achieved under isocratic flow of 0.1% formic acid in 99% H_2O and 1% MeOH at
364 0.250 mL/min through a 100 x 2 mm Polar RP analytical column (Phenomenex®) equipped with
365 a 4 x 3 mm Security Guard Polar-RP™ column (Phenomenex®). Tandem mass spectrometry
366 was operated in positive electrospray ionization (ESI) mode, monitoring mass transitions of
367 256.1 to 152.1 for GCV and 261.2 to 152.1 for the internal standard. Quantification was based
368 on a calibration curve fit with a $1/x^2$ weighted linear regression over the range of 50 to 4000
369 fmol/sample. Intra-day accuracy was within ±4.0% of nominal values and the coefficient of
370 variation (CV) was within 4.9% across three runs with 6 technical replicates each of quality
371 control samples.

372

373 **Clinical range estimate**

374 The clinical range used to guide assay development was derived from the range of
375 concentrations observed in the ValEAR study (233 to 1891 fmol/6 mm punch). Due to the low
376 sample size of participants on valganciclovir used in this dataset, we extended this range to 100

377 to 3200 fmol/6 mm punch, based on the assumption that variability at the upper end of the
378 range would exceed that of the lower end [22]. Assuming that each 6 mm punch holds 17.2 µL
379 of sample based on the storage capacity of Whatman™ 903 Proteinsaver cards, we converted
380 values in fmol/6mm punch to molar concentrations in REACTR. The resulting molar clinical
381 range within the REACTR assay was 0.362 nM to 11.6 nM, accounting for a final blood dilution
382 of 6.25% in the reaction.
383
384 **Data analysis and statistical methods**
385 Enzyme inhibition curves were generated in GraphPad Prism 10 using REACTR fluorescence
386 values at the 60-minute timepoint. When applicable, fluorescence intensities were normalized to
387 the average of the "no drug" positive and "no RT" negative controls as maximum and minimum
388 values, respectively. Curves were fit to four-parameter logistic regression curves. The intra-
389 assay coefficient of variation (CV) was calculated from the baseline-subtracted mean
390 fluorescence of the positive control from 3 technical replicates. The inter-assay CV was
391 calculated from the baseline-subtracted mean fluorescence of the positive control from 3
392 independent replicates, each representing the mean of 3 technical replicates. Intra-assay Z-
393 prime (Z') score was calculated using the raw fluorescence mean and standard deviation values
394 of assay controls from 3 technical replicates. Inter-assay Z-prime (Z') score was calculated
395 using the raw fluorescence mean and standard deviation values of assay controls from 3
396 independent replicates, each representing the mean of 3 technical replicates. All clinical
397 samples were run and analyzed blinded. One-way ANOVA tests with multiple comparisons were
398 performed using GraphPad Prism 10 and the reported p-values were adjusted to account for
399 multiple hypothesis tests. Correlation between LC-MS/MS GCV-TP concentrations and
400 fluorescence were determined using a Pearson's correlation coefficient.
401

402 ## Acknowledgments

403 ***Acknowledgements.*** We would like to credit DBCLS for the centrifuge and thermal cycler icons
404 in Figure 2, which are licensed under CC-BY 4.0 Unported
405 (https://creativecommons.org/licenses/by/4.0/) and Servier for the microtube icons in Figure 2,
406 which are licensed under CC-BY 3.0 (https://creativecommons.org/licenses/by/3.0/) and had the
407 contents and lids modified.
408

Author Contributions. **W.A.C.:** Conceptualization; Formal analysis; Investigation; Methodology; Validation; Writing – original draft; Writing – review & editing; Visualization; Project administration. **M.A.S.:** Conceptualization; Methodology; Writing – review & editing. **C.H.L.:** Methodology. **M.M.C.:** Funding acquisition; Methodology; Writing – review & editing. **C.A.C.:** Methodology. **A.H.P.:** Resources. **J.E.R.:** Resources; Writing – review & editing. **A.O.O:** Conceptualization; Funding acquisition; Methodology; Project administration; Supervision; Resources; Writing – review & editing.

Data Availability. Nucleotide sequences of REACTR reagents are available in supplementary Table 1. Raw and analyzed data are available on Zenodo [37].

Conflicts of Interest. The authors declare the following competing financial interest(s): W.A.C., M.A.S., and A.O.O. are inventors on a patent filed based on this work (63/872,224). M.A.S., M.M.C., and A.O.O. are inventors on patents filed based on related work on enzymatic assays for measuring RT inhibitors (19/396,892, PCT/US2020/037609).

Financial Support. This work was supported by the Arnold and Mabel Beckman Foundation and the Washington Entrepreneurial Research Evaluation and Commercialization Hub (WE-REACH) to A.O.O.

Abbreviations

GCV, Ganciclovir; VGCV, Valganiclovir; GCV-TP, Ganciclovir triphosphate; TDM, Therapeutic drug monitoring; REACTR, REverse transcriptase ACTivity with CRISPR; LC-MS/MS, Liquid chromatography tandem mass spectrometry; HPLC, high-performance liquid chromatography; RT, Reverse transcriptase; cCMV, Congenital cytomegalovirus; NRTI, Nucleotide reverse transcriptase inhibitor; DBS, Dried blood spots.

References

[1] M. Zuhair *et al.*, “Estimation of the worldwide seroprevalence of cytomegalovirus: A systematic review and meta-analysis,” *Reviews in Medical Virology*, vol. 29, no. 3, p. e2034, May 2019, doi: 10.1002/rmv.2034.

[2] P. Ssentongo *et al.*, “Congenital Cytomegalovirus Infection Burden and Epidemiologic Risk Factors in Countries With Universal Screening: A Systematic Review and Meta-analysis,”

JAMA Netw Open, vol. 4, no. 8, p. e2120736, Aug. 2021, doi: 10.1001/jamanetworkopen.2021.20736.

[3] D. W. Kimberlin, R. Banerjee, E. D. Barnett, R. Lynfield, and M. H. Sawyer, Eds., "Cytomegalovirus Infection," in *Red Book: 2024–2027 Report of the Committee on Infectious Diseases*, 33rd ed., American Academy of Pediatrics345 Park Blvd, Itasca, IL 60143, 2024, pp. 344–352. doi: 10.1542/9781610027373-S3_003_015.

[4] M. J. Korndewal, A. M. Oudesluys-Murphy, A. C. M. Kroes, M. A. B. Van Der Sande, H. E. De Melker, and A. C. T. M. Vossen, "Long-term impairment attributable to congenital cytomegalovirus infection: a retrospective cohort study," *Develop Med Child Neuro*, vol. 59, no. 12, pp. 1261–1268, Dec. 2017, doi: 10.1111/dmcn.13556.

[5] S. D. Grosse, P. Fleming, M. H. Pesch, and W. D. Rawlinson, "Estimates of congenital cytomegalovirus-attributable infant mortality in high-income countries: A review," *Reviews in Medical Virology*, vol. 34, no. 1, p. e2502, Jan. 2024, doi: 10.1002/rmv.2502.

[6] E. Forte, Z. Zhang, E. B. Thorp, and M. Hummel, "Cytomegalovirus Latency and Reactivation: An Intricate Interplay With the Host Immune Response," *Front. Cell. Infect. Microbiol.*, vol. 10, p. 130, Mar. 2020, doi: 10.3389/fcimb.2020.00130.

[7] S. R. Permar, M. R. Schleiss, and S. A. Plotkin, "A vaccine against cytomegalovirus: how close are we?," *Journal of Clinical Investigation*, vol. 135, no. 1, p. e182317, Jan. 2025, doi: 10.1172/JCI182317.

[8] A. Lankina, M. Raposo, A. Hargreaves, C. Atkinson, P. Griffiths, and M. B. Reeves, "Developing a Vaccine Against Human Cytomegalovirus: Identifying and Targeting HCMV's Immunological Achilles' Heel," *Vaccines*, vol. 13, no. 5, p. 435, Apr. 2025, doi: 10.3390/vaccines13050435.

[9] J. C. Martin, C. A. Dvorak, D. F. Smee, T. R. Matthews, and J. P. H. Verheyden, "9-(1,3-Dihydroxy-2-propoxymethyl)guanine: a new potent and selective antiherpes agent," *J. Med. Chem.*, vol. 26, no. 5, pp. 759–761, May 1983, doi: 10.1021/jm00359a023.

[10] K. K. Biron *et al.*, "Metabolic activation of the nucleoside analog 9-[(2-hydroxy-1-(hydroxymethyl)ethoxy]methyl)guanine in human diploid fibroblasts infected with human cytomegalovirus.," *Proc. Natl. Acad. Sci. U.S.A.*, vol. 82, no. 8, pp. 2473–2477, Apr. 1985, doi: 10.1073/pnas.82.8.2473.

[11] K. B. Frank, J. F. Chiou, and Y. C. Cheng, "Interaction of herpes simplex virus-induced DNA polymerase with 9-(1,3-dihydroxy-2-propoxymethyl)guanine triphosphate.," *Journal of Biological Chemistry*, vol. 259, no. 3, pp. 1566–1569, Feb. 1984, doi: 10.1016/S0021-9258(17)43446-6.

[12] S. Marfil *et al.*, "Subtherapeutic Exposure of Ganciclovir in Children Despite Appropriate Dosing: A Short Communication," *Therapeutic Drug Monitoring*, vol. 45, no. 2, p. 269, Apr. 2023, doi: 10.1097/FTD.0000000000001050.

[13] J. Leung, S. D. Grosse, B. Yockey, and T. M. Lanzieri, "Ganciclovir and Valganciclovir Use Among Infants With Congenital Cytomegalovirus: Data From a Multicenter Electronic Health Record Dataset in the United States," *Journal of the Pediatric Infectious Diseases Society*, vol. 11, no. 8, pp. 379–382, Aug. 2022, doi: 10.1093/jpids/piac034.

[14] A.-G. Märtson *et al.*, "Therapeutic Drug Monitoring of Ganciclovir: Where Are We?," *Therapeutic Drug Monitoring*, vol. 44, no. 1, pp. 138–147, Feb. 2022, doi: 10/gqmxjv.

[15] K. Hosseini, W. March, F. H. M. Jongsma, F. Hendrikse, and M. Motamedi, "Noninvasive Detection of Ganciclovir in Ocular Tissue by Raman Spectroscopy: Implication for Monitoring of Drug Release," *Journal of Ocular Pharmacology and Therapeutics*, vol. 18, no. 3, pp. 277–285, Jun. 2002, doi: 10.1089/108076802760116197.

[16] S. Saleh and G. Hempel, "Quantification of ganciclovir in human plasma using capillary electrophoresis," *Electrophoresis*, vol. 27, no. 12, pp. 2439–2443, Jun. 2006, doi: 10.1002/elps.200500903.

[17] T. Alinejad, C. Chen, M. Shamsipur, M. Bagher Gholivand, and G. Paimard, “Electrochemical evaluation and determination of antiretroviral drug ganciclovir based on Fe-Cu/TiO2/ multi-walled carbon nanotubes sensor,” *Measurement*, vol. 214, p. 112846, Jun. 2023, doi: 10.1016/j.measurement.2023.112846.

[18] P.-P. Piché-Renaud *et al.*, “Treatment of Congenital Cytomegalovirus and Ganciclovir Therapeutic Drug Monitoring in Twin Preterm Infants,” *The Journal of Pediatric Pharmacology and Therapeutics*, vol. 28, no. 1, pp. 93–101, Jan. 2023, doi: 10.5863/1551-6776-28.1.93.

[19] A. Abu Bakar, H. Payne, N. Tickner, M. A. Muhd Helmi, T. G. Jacobs, and H. Lyall, “Dosing, Toxicity and Drug Concentrations for Ganciclovir/Valganciclovir in Preterm and Low Birthweight Infants Treated for Cytomegalovirus,” *Pediatric Infectious Disease Journal*, vol. 44, no. 4, pp. 319–325, Apr. 2025, doi: 10.1097/INF.0000000000004605.

[20] A. Galar *et al.*, “Valganciclovir—Ganciclovir Use and Systematic Therapeutic Drug Monitoring. An Invitation to Antiviral Stewardship,” *Antibiotics*, vol. 10, no. 1, p. 77, Jan. 2021, doi: 10.3390/antibiotics10010077.

[21] B. M. Ritchie *et al.*, “Relationship of Ganciclovir Therapeutic Drug Monitoring with Clinical Efficacy and Patient Safety,” *Antimicrob Agents Chemother*, vol. 63, no. 3, pp. e01855-18, Mar. 2019, doi: 10.1128/AAC.01855-18.

[22] P.-A. Billat *et al.*, “Plasma and intracellular exposure to ganciclovir in adult renal transplant recipients: is there an association with haematological toxicity?,” *J. Antimicrob. Chemother.*, vol. 71, no. 2, pp. 484–489, Feb. 2016, doi: 10.1093/jac/dkv342.

[23] H. Wiltshire *et al.*, “Pharmacodynamics of Oral Ganciclovir and Valganciclovir in Solid Organ Transplant Recipients,” *Transplantation*, vol. 79, no. 11, pp. 1477–1483, Jun. 2005, doi: 10.1097/01.TP.0000164512.99703.AD.

[24] C. Stockmann, C. M. T. Sherwin, E. D. Knackstedt, A. L. Hersh, A. T. Pavia, and M. G. Spigarelli, “Therapeutic Drug Monitoring of Ganciclovir Treatment for Cytomegalovirus Infections Among Immunocompromised Children,” *Journal of the Pediatric Infectious Diseases Society*, vol. 5, no. 2, pp. 231–232, Jun. 2016, doi: 10.1093/jpids/piw008.

[25] Q.-Y. Li, J. van den Anker, Y.-E. Wu, G.-X. Hao, and W. Zhao, “Optimizing ganciclovir and valganciclovir dosing regimens in pediatric patients with cytomegalovirus infection: a spotlight on therapeutic drug monitoring,” *Expert Review of Clinical Pharmacology*, Aug. 2023, Accessed: Apr. 11, 2025. [Online]. Available: https://www.tandfonline.com/doi/abs/10.1080/17512433.2023.2181161

[26] S. A. Ho, Slavin ,Monica, Roberts ,Jason A., and M. and Yong, “Optimization of Ganciclovir use in allogeneic hematopoietic cell transplant recipients – the role of therapeutic drug monitoring,” *Expert Review of Anti-infective Therapy*, vol. 19, no. 6, pp. 707–718, Jun. 2021, doi: 10.1080/14787210.2021.1851193.

[27] E. K. McCreary, N. Narayanan, T. Tängdén, and A.-G. Märtson, “(Val)ganciclovir Dosing for Cytomegalovirus: Revisiting the 2005 Wiltshire et al. PK/PD target,” *CMI Communications*, p. 105171, Dec. 2025, doi: 10.1016/j.cmicom.2025.105171.

[28] P.-A. Billat *et al.*, “Liquid chromatography tandem mass spectrometry quantitation of intracellular concentrations of ganciclovir and its phosphorylated forms,” *Anal Bioanal Chem*, vol. 407, no. 12, pp. 3449–3456, May 2015, doi: 10.1007/s00216-015-8554-0.

[29] A. O. Olanrewaju *et al.*, “Enzymatic Assay for Rapid Measurement of Antiretroviral Drug Levels,” *ACS Sens.*, vol. 5, no. 4, pp. 952–959, Apr. 2020, doi: 10.1021/acssensors.9b02198.

[30] A. O. Olanrewaju *et al.*, “Pilot evaluation of an enzymatic assay for rapid measurement of antiretroviral drug concentrations,” *Virol J*, vol. 18, no. 1, p. 77, Dec. 2021, doi: 10.1186/s12985-021-01543-x.

[31] A. O. Olanrewaju *et al.*, “REVERSE TRANSCRIPTASE chain termination (RESTRICT) for selective measurement of nucleotide analogs used in HIV care and prevention,”

Bioengineering & Transla Med, vol. 8, no. 1, p. e10369, Jan. 2023, doi: 10.1002/btm2.10369.

[32] C. Brainerd *et al.*, “REverse transcriptase ACTivity (REACT) assay for point-of-care measurement of established and emerging antiretrovirals for HIV treatment and prevention,” Aug. 17, 2024, *Bioengineering*. doi: 10.1101/2024.08.13.607804.

[33] M. A. Singh, M. M. Chang, Q. Wang, C. Rodgers, B. R. Lutz, and A. O. Olanrewaju, “Rapid Enzymatic Assay for Antiretroviral Drug Monitoring Using CRISPR-Cas12a-Enabled Readout,” *ACS Synth. Biol.*, vol. 14, no. 2, pp. 510–519, Feb. 2025, doi: 10.1021/acssynbio.4c00674.

[34] L. Y. Shin *et al.*, “Impact of CMV Therapy With Valganciclovir on Immune Activation and the HIV Viral Load in Semen and Blood: An Observational Clinical Study,” *JAIDS Journal of Acquired Immune Deficiency Syndromes*, vol. 65, no. 3, pp. 251–258, Mar. 2014, doi: 10.1097/01.qai.0000435256.34306.c1.

[35] C. Vanpouille *et al.*, “A common anti-cytomegalovirus drug, ganciclovir, inhibits HIV-1 replication in human tissues ex vivo,” *AIDS*, vol. 31, no. 11, p. 1519, Jul. 2017, doi: 10.1097/QAD.0000000000001532.

[36] B. Lindquist-Kleissler *et al.*, “Intracellular Ganciclovir Triphosphate Concentrations in Children With Congenital Cytomegalovirus Infection,” *The Journal of Infectious Diseases*, p. jiaf633, Dec. 2025, doi: 10.1093/infdis/jiaf633.

[37] W. Chernoske *et al.*, “Dataset for the manuscript ‘REverse-transcriptase ACTivity with CRISPR (REACTR) Assay for Ganciclovir Triphosphate Monitoring.’” Zenodo, Dec. 08, 2025. doi: 10.5281/ZENODO.17860212.

[38] Q. T. Orb *et al.*, “Congenital Cytomegalovirus Testing Outcomes From the ValEAR Trial,” *Otolaryngol Head Neck Surg*, vol. 170, no. 5, pp. 1430–1441, May 2024, doi: 10.1002/ohn.670.

[39] J.-H. Zheng *et al.*, “Application of an intracellular assay for determination of tenofovir-diphosphate and emtricitabine-triphosphate from erythrocytes using dried blood spots,” *Journal of Pharmaceutical and Biomedical Analysis*, vol. 122, pp. 16–20, Apr. 2016, doi: 10.1016/j.jpba.2016.01.038.

[40] L. R. Bushman *et al.*, “Determination of nucleoside analog mono-, di-, and tri-phosphates in cellular matrix by solid phase extraction and ultra-sensitive LC–MS/MS detection,” *Journal of Pharmaceutical and Biomedical Analysis*, vol. 56, no. 2, pp. 390–401, Sep. 2011, doi: 10.1016/j.jpba.2011.05.039.

[41] J. E. Rower, C. Nielson, K. Shi, and A. H. Park, “Validation of an assay for quantifying ganciclovir in dried blood spots,” *J Pharm Biomed Anal*, vol. 184, p. 113181, May 2020, doi: 10.1016/j.jpba.2020.113181.

[42] J.-H. Zhang, T. D. Y. Chung, and K. R. Oldenburg, “A Simple Statistical Parameter for Use in Evaluation and Validation of High Throughput Screening Assays,” *SLAS Discovery*, vol. 4, no. 2, pp. 67–73, Apr. 1999, doi: 10.1177/108705719900400206.